CrossMark

Myxobolus imparfinis n. sp. (Myxozoa: Myxosporea), a new gill parasite of *Imparfinis mirini* Haseman (Siluriformes: Heptapteridae) in Brazil

Diego Henrique Mirandola Dias Vieira · Vinícius Panciera Tagliavini ·
Vanessa Doro Abdallah · Rodney Kozlowiski de Azevedo

Abstract A new species of myxozoan, *Myxobolus imparfinis* n. sp. is described based on material from the gills of *Imparfinis mirini* (Haseman) (Heptapteridae). Mature myxospores are round, measuring 7.1–8.4 (7.9 ± 0.3) μm in length, 4.5–6.2 (5.5 ± 0.5) μm in width and 3.1–4.2 (3.7 ± 0.3) μm in thickness. The polar capsules are of unequal size, the larger polar capsule measuring 3.4–4.5 (3.9 ± 0.3) μm in length and 1.4–2.0 (1.7 ± 0.1) μm in width and the smaller capsule measuring 3.1–3.8 (3.4 ± 0.2) μm in length and 1.2–1.8 (1.5 ± 0.2) μm in width. The polar filament presents 6–7 coils. Spores had a prevalence of infection of 75% (6/8). In histological analyses we detected the development site of spores in primary filaments, in afferent branchial artery, thus classifying the type of infection to the filamental type and vascular subtype. The phylogenetic analyses of a dataset including species *Myxobolus* Bütschli, 1882 and *Henneguya* Thélohan, 1892 from South America recovered *M. imparfinis* n. sp. as a sister species of *Myxobolus flavus* Carriero, Adriano, Silva, Ceccarelli & Maia, 2013. To our knowledge, this is the first record of a myxozoan species parasitising *I. mirini*.

D. H. M. D. Vieira · V. P. Tagliavini
Departamento de Parasitologia, Universidade Estadual Paulista "Júlio de Mesquita Filho" - UNESP, Botucatu, São Paulo, Brazil

V. D. Abdallah · R. K. de Azevedo (✉)
Departamento de Ciências Ambientais, Universidade do Sagrado Coração (USC), Bauru, São Paulo, Brazil
e-mail: azevedork@gmail.com

Introduction

Myxozoans are parasites of the phylum Cnidaria Hatschek, 1888 that can be pointed out as some of the main causative agents of fish injuries. The most diverse genus within the Class Myxosporea Buetchli, 1881 is *Myxobolus* Bütschli, 1882 comprising species which parasitise mainly fishes (Eiras et al., 2014). The importance of the study of myxozoans was evidenced by Barassa et al. (2003), who showed that some species can cause serious problems to their hosts, resulting in high mortality rates.

Fishes belonging to the order Siluriformes (Nelson) are perhaps the most well represented in South America, with about 1,056 species described (Buckup et al., 2007). *Imparfinis mirini* (Haseman), belongs to the family Heptapteridae (Gill), a large, diversified and well-distributed fish group in the Neotropical region (Ferraris, 2007).

The use of molecular data in conjunction with morphological analysis has been used to describe new species of myxozoans (e.g. Carriero et al., 2013;

Capodifoglio et al., 2016). The main goal of this study was to describe a new species of *Myxobolus*, found in the gills of *I. mirini* during a parasitological survey, based on light microscopy, histology and assessment of its phylogenetic relationships with other representatives of the family Myxobolidae Thélohan, 1892 from South America.

Materials and methods

In August 2016, specimens of *I. mirini* (n = 8; total length of 6.2–7.0 cm, weight of 1.98–2.4 g; 6 females/ 2 males), were collected in River Batalha (22°29′04.6″S, 49°03′53.3″W), Agudos, São Paulo, Brazil. Fish were collected using sieves and euthanised by neural pithing immediately after capture. Gills, heart, liver, gonad, stomach, intestine, bone marrow, kidney, swim bladder and gall-bladder fresh smears were observed under a differential interference contrast microscope (Leica DMLB 5000, Leica Microsystems, Wetzlar, Germany) at a magnification of 1000×. Gill samples of infected fish were collected and fixed according to the protocols for further morphological and molecular analysis.

Spore length, width and thickness, polar capsule length, width and the number of turns of the polar filament were measured following the recommendations of Lom & Arthur (1989). Measurements of 30 spores from gills of 6 infected fish were taken from digital images at a magnification of 1000×, under light microscopy with Leica software application suite LAS V3.8 (Leica Microsystems, Wetzlar, Germany). Schematic representation of mature spores was made using the software CorelDRAW® (Corel Draw Graphics Suite, version x8, Corel Corporation, Canada). All measurements are in micrometres and are presented as the range followed by the mean and standard deviation in parentheses.

Infected gills collected for histological analysis were placed into a 5% formaldehyde, dehydrated in an ethanol series (3× into 70% every 2 h and then 95% for 4 h). The material was then immersed in a mixture (50% resin and 50% ethanol) for 12 h and embedded in resin (HistoResin, Leica, Wetzlar, Germany). Finally, 3 μm sections were made, stained with hematoxylin-eosin and observed under a light microscope.

Samples of two infected gills were fixed in absolute ethanol for DNA extraction. The DNA extraction followed the animal tissue protocol DNeasy Blood & Tissue Kit (Qiagen, Hilden, Germany). The SSU rDNA gene was amplified using different primer combinations and PCR conditions (Table 1). Amplifications were performed using a Bio-Rad Mycycler personal thermal cycler (Bio-Rad Laboratories Pty Ltd., Gladesville, Australia), with initial denaturation at 94°C for 3 min, followed by 28–34 cycles of 94°C for 40 s, specific annealing temperature for 40 s, 72°C for 2 min, and a final extension at 72°C for 10 min. PCR reactions were performed in 25 μl reactions containing 3 μl of DNA extract, 1 μl of each PCR primer using Ready-to-Go PCR beads (Pure Taq[TM]-Ready-to-Go[TM] beads, GE Healthcare, Chicago, USA), the solution consisted of stabilizers, BSA, dATP, dCTP, dGTP, dTTP, ± 2.5 units of puReTaq DNA polymerase and reaction buffer. Each bead was reconstituted to a final volume of 25 μl and the concentration of each dNTP was 200 μM in 10 mM Tris-HCl (pH 9.0 at room temperature), 50 mM KCl and 1.5 mM $MgCl_2$. After checking for the presence of the expected DNA amplicons in a 1% agarose gel in TAE buffer, PCR products were cleaned up using QIAquick PCR Purification Kit (Qiagen®, CA, USA). Automated sequencing was performed directly on the purified PCR products from specimens using BigDye v.3.1 Terminator Cycle Sequencing Ready Reaction kit (Applied Biosystems, Foster City, CA, USA) for cycle sequencing. Sequences were run on an Applied Biosystems ABI 3500 DNA genetic analyzer, edited in Sequencher[TM] v. 5.2.4 (Gene Codes, Ann Arbor, MI) and subjected to BLAST analyses (http://blast.ncbi. nlm.nih.gov).

The newly generated sequences of partial SSU rDNA were aligned using Geneious version 7.1.3 (Kearse et al., 2012) with ClustalW algorithm (Larkin et al., 2007) and default settings with related sequences for species of *Myxobolus* and *Henneguya* Thélohan, 1892 from South America retrieved from GenBank. *Myxydium ceccarellii* Adriano, Silva, Atkinson, Bartholomew & Maia, 2014 (KJ499821) was used as the outgroup.

All analyses were performed using only positions that were unambiguously alignable across all taxa (621 nt). The JModelTest 2.1.1 program (Posada, 2008) was used to select the most appropriate evolutionary model for Maximum Likelihood (ML) and Bayesian inference (BI) analyses. The best-fitting model of nucleotide substitution was GTR + I + G

Table 1 Primers used to amplify SSU rDNA in this study

Primer[a]	Sequence 5′-3′	PCR round	Reference
Erib1	ACCTGGTTGATCCTGCCAG	First	Barta et al. (1997)
Erib10	CTTCCGCAGGTTCACCTACGG	First	Barta et al. (1997)
MyxospecF	TTCTGCCCTATCAACTTGTTG	Nested	Fiala (2006)
MX5	CTGCGGACGGCTCAGTAAATCAGT	Nested	Andree et al. (1997)
MyxospecR	GGTTCNCDGRGGGMCCAAC	Nested	Fiala (2006)

[a]Amplicon size *c*.1,000 nt

based on the Akaike Information Criterion (AIC). Node support for ML was determined by performing 1,000 bootstrap replicates.

Bayesian inference (BI) analysis was performed using MrBayes 3.1.2 (Ronquist & Huelsenbeck, 2003). Markov Chain Monte Carlo (MCMC) chains were run for 10 million generations and the log-likelihood scores plotted. The 'burn in' was set to 25%. Phylogenetic trees were generated and edited in FigTree v1.4 (Rambaut, 2012). An alignment containing only trimmed sequences of *Myxobolus* spp. parasitising fishes in South America was used to produce a distance matrix.

Family Myxobolidae Thélohan, 1892
Genus *Myxobolus* Bütschli, 1882

Myxobolus imparfinis n. sp.

Type-host: *Imparfinis mirini* (Haseman) (Siluriformes: Heptapteridae).
Type-locality: River Batalha (22°29′04.6″S 49°03′53.3″W), municipality of Agudos, State of São Paulo, Brazil.
Type-material: Hapantotype (a slide containing fresh spores) was deposited in the Myxozoa Type Slide Collection at the Instituto Nacional de Pesquisa da Amazônia (INPA), Manaus, Brazil under the accession number INPA 31. Histological sections of gills containing spores were also deposited in the collection of the Museum of Zoology "Adão José Cardoso", Institute of Biology, University of Campinas (UNI-CAMP), São Paulo, Brazil (under the accession number ZUEC-MYX 68).
Site in host: Gills, located in the primary and middle third of the primary gill filaments and developed in the afferent branchial artery.

Prevalence: 75% (in 6 out of 8 fish examined).
Representative DNA sequences: Two SSU rDNA sequences obtained from spores of *M. imparfinis* n. sp. (1,095 and 1,051 nt; GenBank: MF425815 and MF425816, respectively)
ZooBank registration: To comply with the regulations set out in article 8.5 of the amended 2012 version of the *International Code of Zoological Nomenclature* (ICZN, 2012), details of the new species have been submitted to ZooBank. The Life Science Identifier (LSID) for *Myxobolus imparfinis* n. sp. is urn:lsid:-zoobank.org:act:17D4A604-104D-48E3-8D8E-0708 610FE639.
Etymology: The specific name (*imparfinis*) is derived from the genus of the host.

Fig. 1 Light photomicrographs of mature spores of *Myxobolus imparfinis* n. sp. from the gills of *Imparfinis mirini*. *Scale-bar*: 5 μm
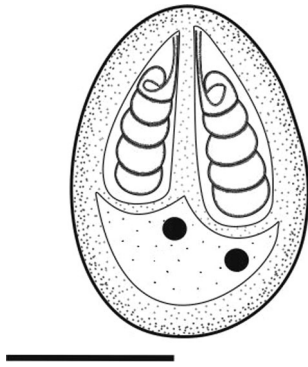
Fig. 2 Schematic representation of a mature spore of *Myxobolus imparfinis* n. sp. *Scale-bar*: 3 μm

Description (Figs. 1, 2, 3, 4)

Spores[Based on 30 spores.] Spores round, with binucleate sporoplasm. Mature spores from gills 7.1–8.4 (7.9 ± 0.3) long, 4.5–6.2 (5.5 ± 0.5) wide 3.1–4.2 (3.7 ± 0.3) thick. Polar capsules 2, of unequal size; larger polar capsule 3.4–4.5 (3.9 ± 0.3) long, 1.4–2.0 (1.7 ± 0.1) wide; smaller pollar capsule 3.1–3.8 (3.4 ± 0.2) long, 1.2–1.8 (1.5 ± 0.2) wide. Polar filament with 6–7 coils (Figs. 1–2).

Remarks

The morphology of the myxospores found in the gills of *I. mirini* corresponded to the genus *Myxobolus* following Lom & Dyková (2006), based on rounded

spores containing two polar capsules and a binucleated sporoplasm. The morphology of *M. imparfinis* n. sp. was compared to other species of *Myxobolus* that parasite fishes, mainly from South America. The greater focus of comparison concerned *Myxobolus* spp. that parasitise fishes of the Order Siluriformes (Table 2).

Of the five species (see Table 2 for details), four are parasitic in the gills of their hosts (*Myxobolus flavus* Carriero, Adriano, Silva, Ceccarelli & Maia, 2013; *Myxobolus niger* Mathews, Maia & Adriano, 2016; *Myxobolus sciades* Azevedo, Casal, Mendonça, Carvalho, Matos & Matos, 2010 and *Myxobolus cordeiroi* Adriano, Arana, Alves, Silva, Ceccareli, Henrique-Silva & Maia, 2009) and one is parasitic in the opecular cavity of its host (*Myxobolus absonus* Cellere, Cordeiro & Adriano, 2002). *Myxobolus flavus* resembles morphologically *M. imparfinis* n. sp., but all morphometric features are larger than in the new species. *Myxobolus niger*, *M. absonus*, *M. sciades* and *M. cordeiroi* exhibit larger spore length than *M. imparfinis* n. sp. (means 11.3 ± 0.4 μm, 15.7 ± 1.5 μm, 9.15 ± 0.39 μm and 10.8–11.3 μm, respectively *vs* 7.9 ± 0.3 μm). In addition, only *M. absonus* has polar capsules of different sizes as in the new species; however both polar capsules are longer than the polar capsules of *M. imparfinis* n. sp. (larger capsule mean 6.4 ± 0.7 μm *vs* 3.9 ± 0.3 μm; smaller capsule mean 4.2 ± 0.6 μm *vs* 3.4 ± 0.2 μm).
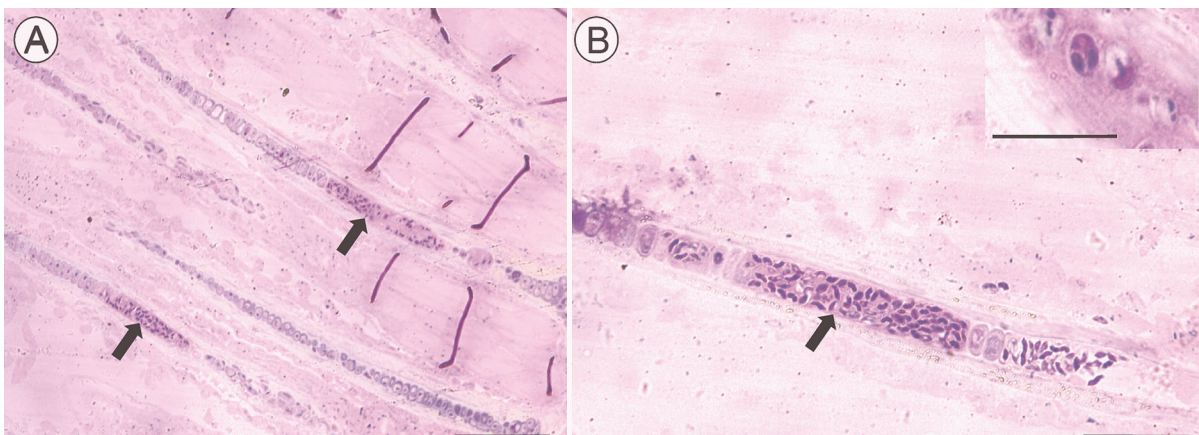

Fig. 3 Photomicrographs of histological sections of gills infected with *Myxobolus imparfinis* n. sp. A, Histological section of gill filaments from *Imparfinis mirini* infected with spores of *M. imparfinis* in the afferent branchial artery (*arrows*); B, Enlarged image of spores (*arrow*) developed in afferent branchial artery of a primary gill filament. Inset: detail of spore of *M. imparfinis* n. sp. *Scale-bars*: A, 100 μm; B, 50 μm (inset, 20 μm)
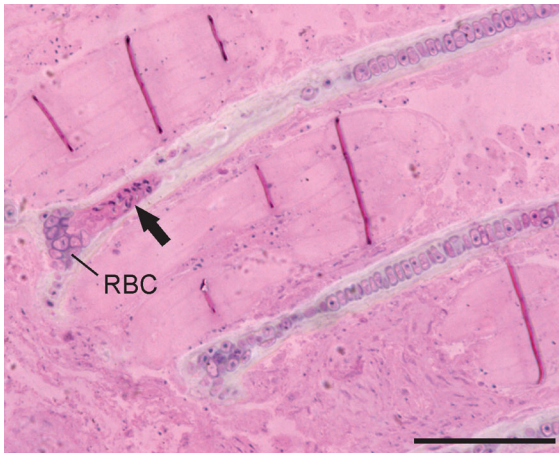
Fig. 4 Photomicrographs of histological sections of gills infected with *Myxobolus imparfinis* n. sp. showing spores (*arrow*) located at the beginning of the lumen of the afferent branchial artery blocking the passage of red blood cells (RBC). *Scale-bar*: 100 μm

Comparisons were also made with *Myxobolus* spp. that parasitise fishes of other orders. The species most resembling *M. imparfinis* n. sp. is *Myxobolus brycon* Azevedo, Casal, Marques, Silva & Matos, 2011, but this species has a smaller body width compared with *M. imparfinis* n. sp.: 3.9–4.8 (4.2 ± 0.5) μm *vs* 4.5–6.2 (5.5 ± 0.5) 4.54–6.17 μm. In addition, the polar filament in *M. brycon* presents 8–9 turns (*vs* 6–7 turns in *M. imparfinis* n. sp.) (see Azevedo et al., 2011).

When compared to *Myxobolus* species from other geographical regions, the species that most closely resembles *M. imparfinis* n. sp. was *Myxobolus omari* Székely, Shaharom-Harrison, Cech, Mohamed & Molnár, 2009. However, *M. omari* has a body width of 12 μm, which is much larger when compared with *M. imparfinis* n. sp. (5.5 ± 0.5 μm) (see Székely et al., 2009). All other species that were compared did not show morphological or morphometric characteristics resembling *M. imparfinis* n. sp. Each species verified presented at least one morphometric feature or number of turns of the polar filament significantly different when compared with the new species.

Histological analysis

The histological analysis of gills of *I. mirini* revealed that the spores developed in the intralamellar gill regions. The spores were located in the primary and middle third of the primary gill filaments and developed in the afferent branchial artery (Fig. 3A–B). Histological sections also showed the presence of spores at the beginning of the lumen of the afferent branchial artery, blocking the passage of red blood cells of the host (Fig. 4). However, we did not observe any inflammatory influence, secondary infections, mucus production or even deformations of the lamellae in the gills of *I. mirini*.

Molecular and phylogenetic analysis

We amplified a fragment of the SSU rDNA gene from spores collected from the gills of two infected *I. mirini* (1,051 and 1,095 nt long); when aligned the sequences showed a similarity of 99.5%. The BLAST search using the partial SSU rDNA sequence data for *M. imparfinis* n. sp. did not match any myxozoan sequence available on GenBank. The newly generated sequence (1,095 nt long) was most similar to that for *M. flavus* (divergence of 12.1%, Table 3).

The generated ML and BI trees showed an identical topology, therefore, only the BI tree is presented here. In these solutions, the South American species of *Myxobolus* and *Henneguya* clustered into two clades, one composed only of *Myxobolus* spp. and the other composed of species of *Myxobolus* and *Henneguya*. It was possible to observe the formation of a paraphyletic group formed by the genera *Henneguya* and *Myxobolus*. *Myxobolus imparfinis* n. sp. appeared as a sister species of M. *flavus* (Fig. 5).

In the clade composed by species of *Myxobolus* and *Henneguya*, a clustering by host specificity was observed. The species were divided into two major groups, one composed only of myxozoan parasites of siluriform fishes and the other group composed only of myxozoan parasites of characiform fishes. In the clade composed only of *Myxobolus* spp., all species are parasites of characiform fishes; however the same pattern of host specificity clustering was observed in relation to the host family. The species were divided into two major groups, one composed only of *Myxobolus* spp. parasitising fishes of the family Prochilodontidae (Castro & Vari) and the other group composed only of myxozoan parasites of fishes of the family Bryconidae (Eigenmann).

Table 2 Comparative data for *Myxobolus imparfinis* n. sp. and *Myxobolus* spp. from siluriform fishes in South America

Species	Spore length	Spore width	Thickness	LPC	WPC	NCF	Site in host	Host	Reference
M. imparfinis n. sp.	7.1–8.4 (7.9 ± 0.3)	4.5–6.2 (5.5 ± 0.5)	3.1–4.2 (3.7 ± 0.3)	3.4–4.5 (3.9 ± 0.3)[a]; 3.1–3.8 (3.4 ± 0.2)[b]	1.4–2.0 (1.7 ± 0.1)[a]; 1.2–1.8 (1.5 ± 0.2)[b]	6–7	Gills (primary gill filaments and developed in the afferent branchial artery)	*Imparfinis mirini* (Haseman)	This study
M. flavus Carriero, Adriano, Silva, Ceccarelli & Maia, 2013	9.2 ± 0.2	6.5 ± 0.3	4.2 ± 0.2	4.5 ± 0.2	1.6 ± 0.1	4–5	Gills	*Pseudoplatystoma corruscans* (Spix & Agassiz)	Carriero et al. (2013)
M. niger Mathews, Maia & Adriano, 2016	11.3 ± 0.4	6.8 ± 0.2	4.1 ± 0.2	5.0 ± 0.3	2.0 ± 0.1	6–7	Gills	*Corydoras melini* (Lönnberg & Rendahl)	Mathews et al. (2016)
M. absonus Cellere, Cordeiro & Adriano, 2002	15.7 ± 1.5	10.2 ± 0.7	–	6.4 ± 0.7[a]; 4.2 ± 0.6[b]	3.6 ± 0.5[a]; 2.5 ± 0.5[b]	3–5	Opecular cavity	*Pimelodus maculatus* (Lacepède)	Cellere et al. (2002)
M. sciades Azevedo, Casal, Mendonça, Carvalho, Matos & Matos, 2010	9.2 ± 0.4	4.4 ± 0.2	2.6 ± 0.3	4.4 ± 0.4	1.4 ± 0.4	9–10	Gills	*Sciades herzbergii* (Bloch)	Azevedo et al. (2010)
M. cordeiroi Adriano, Arana, Alves, Silva, Ceccareli, Henrique-Silva & Maia, 2009	10.8–11.3	7.1–7.5	5.2–5.6	5.2–5.4	1.4–1.5	5–6	Gills, skin, urinary bladder, serosa and eyes	*Zungaro jahu* (Ihering)	Adriano et al. (2009)

[a]Larger capsule; [b]Smaller capsule. *Abbreviations:* LPC, length of polar capsules; WPC, width of polar capsules; NCF, number of coils of polar filaments

Table 3 Divergence in SSU rDNA sequences of *Myxobolus* spp., parasites of fishes in South America. Data below the diagonal represent the number of different nucleotides; data above the diagonal represent the percent nucleotide divergence (p-distance model)

| Species	1	2	3	4	5	6	7	8	9	10	11	12	13	14	15	16
1 *Myxobolus imparfinis* n. sp.		12.1	29.5	20.5	18.3	18.9	19.4	30.7	32.8	32.3	28.1	30.3	30.2	29.3	34.8	34.6
2 *Myxobolus flavus*	75		29.3	19.7	19.3	19.0	19.7	30.3	32.8	32.9	29.9	31.2	30.8	30.0	34.2	33.2
3 *Myxobolus cordeiroi*	189	189		29.2	27.2	27.6	27.6	27.9	29.2	30.0	26.9	30.7	29.2	31.4	34.1	33.5
4 *Myxobolus cf. cuneus*	128	24	188		17.7	17.3	15.9	21.3	32.3	32.2	28.6	31.4	30.1	29.3	35.2	34.1
5 *Myxobolus pantanalis*	113	120	174	110		15.2	14.6	28.6	31.3	31.1	29.0	29.8	27.7	28.9	35.1	35.2
6 *Myxobolus oliveirai*	118	120	177	108	95		3.7	29.6	30.5	31.6	28.2	31.1	30.0	31.0	33.8	34.2
7 *Myxobolus filamentum*	121	124	177	99	91	23		30.1	30.7	31.5	28.1	31.0	29.9	30.8	33.9	34.3
8 *Myxobolus umidus*	190	189	179	196	177	186	189		26.4	14.8	22.0	22.4	18.3	25.0	29.8	31.1
9 *Myxobolus piraputangae*	206	208	188	204	193	196	194	101		12.5	23.3	25.0	21.0	26.9	27.3	27.8
10 *Myxobolus hilarii*	201	207	192	202	193	198	197	90	76		22.0	26.1	19.7	26.5	29.9	19.6
11 *Myxobolus macroplasmodialis*	176	189	172	179	181	177	176	138	147	137		22.5	21.5	25.5	28.7	27.9
12 *Myxobolus cf. colossomatis*	189	196	198	197	186	190	196	138	155	161	141		20.2	23.3	27.6	28.4
13 *Myxobolus aureus*	187	193	187	188	171	188	187	111	129	120	134	124		24.6	27.4	28.3
14 *Myxobolus porofilus*	182	189	202	183	180	195	194	156	169	166	159	145	153		21.9	22.4
15 *Myxobolus prochilodus*	220	218	220	223	222	214	215	189	171	188	180	172	173	138		7.3
16 *Myxobolus curimatae*	220	213	217	217	224	218	219	192	175	187	176	178	180	142	44	
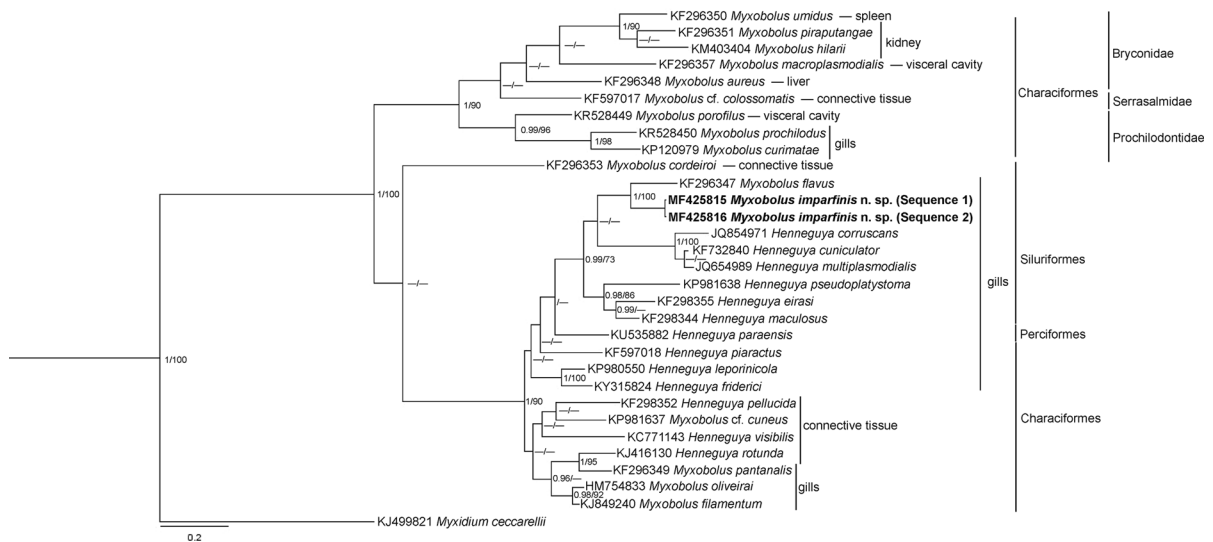
Fig. 5 Maximum likelihood (ML) phylogenetic tree based on partial SSU rDNA sequences showing the position of *Myxobolus imparfinis* n. sp. among other species of *Myxobolus*/*Henneguya* from South America. Numbers at the nodes represent Bayesian posterior probability (BI) and ML bootstrap values (BI/ML); only values > 0.95 (BI) and 70% (ML) are shown. The scale-bar indicates the distances in substitutions per site

Discussion

Recent studies have shown that myxozoan parasites tend to cluster by tissue tropism in the host (Andree et al., 1999). *Myxobolus imparfinis* n. sp. was resolved as the sister species of the gill parasite *M. flavus* within the clade containing representatives of the two genera. The sequences of the two species showed a difference of 12.1% (75 nt). The interspecific divergence within *Myxobolus* ranged between 0.1%–3.0% thus supporting the distinct status of the new species (Andree et al., 1999). *Henneguya* spp. that parasitise gills of siluriform fishes, such as *Henneguya corruscans* Eiras, Takemoto & Pavanelli, 2009 from the gills of *Pseudoplatystoma corruscans* (Spix & Agassiz), *Henneguya cuniculator* Naldoni, Maia, da Silva & Adriano, 2014 from the gills of *P. corruscans* and *Henneguya multiplasmodialis* Adriano, Carriero, Maia, Silva, Naldoni, Ceccareli & Arana, 2012 from the gills of *P. corruscans* and *Pseudoplatystoma reticulatum* (Eigenmann & Eigenmann), also clustered in this clade.

Mainly due to the artificiality of morphometric characters, Myxozoa are known to include several paraphyletic and polyphyletic taxa (Fiala, 2006). The clustering of myxozoans in clades by host order and host family observed shows a tendency that parasites

of the genus *Myxobolus* and *Henneguya* had a polyphyletic origin with the host specificity influencing parasitism (Capodifoglio et al., 2016).

The histological analysis of the gills of *I. mirini* infected with spores of *M. imparfinis* n. sp. following the terminology proposed by Molnár (2002), we were able to classify the infection being of the filamental type and vascular subtype. According to Molnár (2002), this type is one of the most common plasmodium development, although we did not observe the formation of plasmodia. Adriano et al. (2005) showed that massive myxozoan infections could compromise gill functions by deforming the lamellar structures and reducing the gill area. However, in the present study it was not possible to observe any apparent damage to the host caused by *M. imparfinis* n. sp.

The differences in spore morphology and morphometry and SSU rDNA gene sequences obtained in the present study tend to justify the distinct status of the new species. This contributes to the knowledge of the biodiversity of myxozoans in Brazil and of myxozoans in rarely parasitised fish gill tissues, such as the afferent branchial artery. To the best of our knowledge, *M. imparfinis* n. sp. is the first myxozoan species described and the first record of a myxozoan

species parasitising species of the genus *Imparfinis* and *I. mirini*.

Compliance with ethical standards

Conflict of interest The authors declare that they have no conflict of interest.

Ethical approval All applicable institutional, national and international guidelines for the care and use of animals were followed.

References

Adriano, E. A., Arana, S., Alves, A. L., Silva, M. R. M. D., Ceccarelli, P. S., Henrique-Silva, F., & Maia, A. A. M. (2009). *Myxobolus cordeiroi* n. sp., a parasite of *Zungaro jahu* (Siluriformes: Pimelodiade) from Brazilian Pantanal: morphology, phylogeny and histopathology. *Veterinary Parasitology, 162,* 221–229.

Adriano, E. A., Arana, S., & Cordeiro, N. S. (2005). Histophatology and ultrastructure of *Henneguya caudalongula* sp. n. infecting *Prochilodus lineatus* (Pisces: Prochilodontidae) cultivated in the state of São Paulo, Brazil. *Memórias do Instituto Oswaldo Cruz, 100,* 177–181.

Andree, K. B., Gresoviac, S. J., & Hedrick, R. P. (1997). Small subunit ribosomal RNA sequences unite alternate actinosporean and myxosporean stages of *Myxobolus cerebralis* the causative agent of whirling disease in salmonid fish. *Journal of Eukaryotic Microbiology, 44,* 208–215.

Andree, K. B., Székely, C., Molnár, K., Gresoviac, S. J., & Hedrick, R. P. (1999). Relationships among members of the genus *Myxobolus* (Myxozoa: Bilvalvidae) based on small subunit ribosomal DNA sequences. *Journal of Parasitology, 85,* 68–74.

Azevedo, C., Casal, G., Marques, D., Silva, E., & Matos, E. (2011). Ultrastructure of *Myxobolus brycon* n. sp. (Phylum Myxozoa), parasite of the Piraputanga fish *Brycon hilarii* (Teleostei) from Pantanal (Brazil). *Journal of Eukaryotic Microbiology, 58,* 88–93.

Azevedo, C., Casal, G., Mendonça, I., Carvalho, E., Matos, P., & Matos, E. (2010). Light and electron microscopy of *Myxobolus sciades* n. sp. (Myxozoa), a parasite of the gills of the Brazilian fish *Sciades herzbergii* (Block, 1794) (Teleostei: Ariidae). *Memórias do Instituto Oswaldo Cruz, 105,* 203–207.

Barassa, B., Adriano, E. A., Arana, S., & Cordeiro, N. S. (2003). *Henneguya curvata* sp. n. (Myxosporea: Myxobolidae) parasitizing the gills of *Serrasalmus spilopleura* (Characidae: Serrasalmidae), a South American freshwater fish. *Folia Parasitologica, 50,* 151–153.

Barta, J. R., Martin, D. S., Liberator, P. A., Dashkevicz, M., Anderson, J. W., Feigner, S. D., et al. (1997). Phylogenetic relationships among eight *Eimeria* species infecting domestic fowl inferred using complete small subunit ribosomal DNA sequences. *Journal of Parasitology, 83,* 262–271.

Buckup, P. A., Menezes, N. A., & Ghazzi, M. S. (2007). *Catálogo das espécies de peixes de água doce do Brasil*. Rio de Janeiro: Museu Nacional, Universidade Federal do Rio de Janeiro.

Capodifoglio, K. R., Adriano, E. A., Milanin, T., Silva, M. R., & Maia, A. A. (2016). Morphological, ultrastructural and phylogenetic analyses of *Myxobolus hilarii* n. sp. (Myxozoa, Myxosporea), a renal parasite of farmed *Brycon hilarii* in Brazil. *Parasitology International, 65,* 184–190.

Carriero, M. M., Adriano, E. A., Silva, M. R., Ceccarelli, P. S., & Maia, A. A. (2013). Molecular phylogeny of the *Myxobolus* and *Henneguya* genera with several new South American species. *PLoS One, 8,* e73713.

Cellere, E. F., Cordeiro, N. S., & Adriano, E. A. (2002). *Myxobolus absonus* sp. n. (Myxozoa: Myxosporea) parasitizing *Pimelodus maculatus* (Siluriformes: Pimelodidae), a South American freshwater fish. *Memórias do Instituto Oswaldo Cruz, 97,* 79–80.

Eiras, J. C., Zhang, J. Y., & Molnár, K. (2014). Synopsis of the species of *Myxobolus butschli*, 1882 (Myxozoa: Myxosporea: Myxobolidae) described between 2005 and 2014. *Systematic Parasitology, 88,* 11–36.

Ferraris, C. J. (2007). Checklist of catfishes, recent and fossil (Osteichthyes: Siluriformes), and catalogue of siluriformes primary types. *Zootaxa, 1418,* 180–356.

Fiala, I. (2006). The phylogeny of myxosporea (myxozoa) based on small subunit ribosomal RNA gene analysis. *International Journal for Parasitology, 36,* 1521–1534.

ICZN (2012). *International Commission on Zoological Nomenclature*: Amendment of articles 8, 9, 10, 21 and 78 of the International Code of Zoological Nomenclature to expand and refine methods of publication. *Bulletin of Zoological Nomenclature, 69,* 161–169.

Kearse, M., Moir, R., Wilson, A., Stones-Havas, S., Cheung, M., Sturrock, S., et al. (2012). Geneious Basic: an integrated and extendable desktop software platform for the organization and analysis of sequence data. *Bioinformatics, 28,* 1647–1649.

Larkin, M. A., Blackshields, G., Brown, N. P., Chenna, R., McGettigan, P. A., McWilliam, H., et al. (2007). Clustal W and Clustal X version 2.0. *Bioinformatics, 23,* 2947–2948.

Lom, J., & Arthur, J. R. (1989). A guideline for the preparation of species descriptions in Myxosporea. *Journal of Fish Diseases, 12,* 151–156.

Lom, J., & Dyková, I. (2006). Myxozoa genera: Definition and notes on taxonomy, life cycle terminology and pathogenic species. *Folia Parasitologica, 53,* 1–36.

Mathews, P. D., Maia, A. A., & Adriano, E. A. (2016). Morphological and ultrastructural aspects of *Myxobolus niger* n. sp. (Myxozoa) gill parasite of *Corydoras melini* (Siluriformes: Callichthyidae) from Brazilian Amazon. *Acta Tropica, 158,* 214–219.

Molnár, K. (2002). Site preference of fish myxosporeans in the gill. *Diseases of Aquatic Organisms, 48,* 197–207.

Posada, D. (2008). jModelTest: phylogenetic model averaging. *Molecular Biology and Evolution, 25,* 1253–1256.

Rambaut, A. (2012). FigTree v1.4. Molecular evolution, phylogenetics and epidemiology. http://tree.bio.ed.ac.uk/software/figtree/05/2017. Accessed 24 April 2017.

Ronquist, F., & Huelsenbeck, J. P. (2003). MrBayes 3: Bayesian phylogenetic inference under mixed models. *Bioinformatics, 19,* 1572–1574.

Székely, C., Shaharom-Harrison, F., Cech, G., Mohamed, K., & Molnár, K. (2009). Myxozoan pathogens of Malaysian fishes cultured in ponds and net-cages. *Diseases of Aquatic Organisms, 83,* 49–57.